Study on Mixed-Mode Fracture Characterization in Functionally Graded Materials

D. L. Liu,[1] X. F. Yao,[1] Y. J. Ma,[1] W. Xu[2]

[1]*Department of Engineering Mechanics, AML, Tsinghua University, Beijing 100084, China*
[2]*Department of Engineering Mechanics, Faculty of Civil Engineering and Architecture, Kunming University of Science and Technology, Kunming 650093, China*

Received 30 July 2010; accepted 29 April 2011
DOI 10.1002/app.34815
Published online 24 August 2011 in Wiley Online Library (wileyonlinelibrary.com).

ABSTRACT: The fracture characterizations on mixed-mode crack of functionally graded materials (FGMs) are investigated using digital speckle correlation method (DSCM). The stress intensity factors at mixed-mode crack tip are obtained from digital speckle displacements fields. In combination with finite elements simulation results, the influences of gradient coefficients on fracture behavior of mixed-mode cracks are analyzed. All the results show that the influence of gradient coefficients on fracture modes is not noticeable, and the stress intensity factor at the crack tip in graded materials are clearly influenced by the gradient coefficients, i.e., the stress intensity factors decrease with the increasing of gradient coefficients. © 2011 Wiley Periodicals, Inc. J Appl Polym Sci 123: 2467–2475, 2012

Key words: functionally graded materials; digital speckle correlation method; mechanical properties; fracture; crazing

INTRODUCTION

In recent years, functionally graded materials (FGMs) are widely used in many engineering structures due to the gradual variation of its mechanical properties.[1–4] However, experimental investigations of fracture behavior of FGMs are limited due to the high cost and elaborate facilities required for processing FGMs.[5–7] A few finite elements methods have also been used to simulate fracture behavior of the cracked FGMs.[8,9]

The digital speckle correlation method (DSCM) is to compare two images of the specimen in the undeformed and the deformed state, which has been intensively and widely used in deformation measurement of material and structure.[10–13] The key to this experimental method is to search for the maximum correlation between small zones in the target and the reference images, from which the displacements at different positions in the zone of interest can be obtained. The simplest image-matching procedure in DSCM is cross-correlation, which can determine the in-plane displacement field (u, v) by matching different zones of two images.[14] Recently, many research works were concentrated on improving the accuracy of displacement field and removing the noise from the displacement field. Bruck et al.[15] obtained the higher accuracy using bicubic spline interpolation. Jin et al.[16–19] reported the compensation method for strain field measurements in DSCM. Sutton et al.[20] developed finite elements smoothing technique with one-dimensional generalized cross-validation algorithm to smooth the displacement data. Jin et al.[21] studied mixed-mode fracture response of ZrO_2/NiCr FGMs using fracture test, digital image correlation technique, and extended finite element method.

In this article, fracture characterizations of the mixed-mode crack in the graded material are investigated using DSCM in combination with finite element method. The influences of the gradient coefficients on fracture behavior of the mixed-mode crack are analyzed.

EXPERIMENTAL PRINCIPLE OF DSCM

Figure 1 is the schematic configuration of the experimental setup for digital speckle correlation technology, which consists of a charge-coupled-device (CCD) camera, optical fiber cold light source, image card, digital image correlation processing software written in C++ language, and a personal computer. In this test, the cold light source was used to illuminate the specimen surface. The CCD camera was

Correspondence to: X. F. Yao (yxf@mail.tsinghua.edu.cn).
Contract grant sponsor: NSFC; contract grant number: 10372048.
Contract grant sponsor: Science Foundation of Tsinghua University; contract grant number: JC2003035.
Contract grant sponsor: Start foundation of Overseas-Return People in Ministry of Education of China.

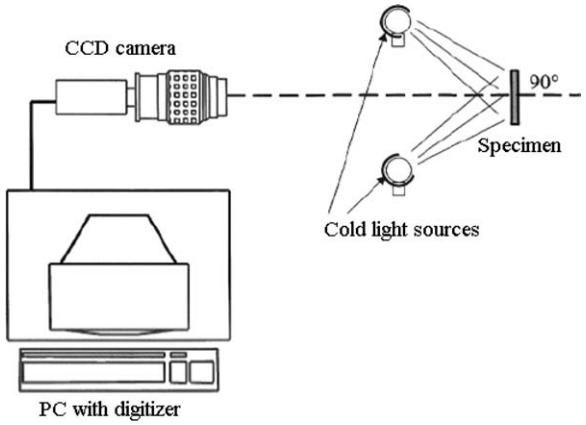

Figure 1 Schematic diagram of digital speckle correlation technology.

used to record the speckle image of the specimen with a resolution of 1280 × 1024 pixels. Then, the image data was saved to a hard disk. After the correlation calculation of two images before and after deformation is performed, the full-field displacements of the specimen surface are obtained.

A correlation equation will be used to search the peak value and improve the measurement accuracy, which is shown in eq. (1).[16,17]

$$C = \frac{\Sigma_{i=1}^{m_s}\Sigma_{j=1}^{m_s}[f(x_i,y_j)-\bar{f}][g(x_i^*,y_j^*)-\bar{g}]}{\sqrt{\Sigma_{i=1}^{m_s}\Sigma_{j=1}^{m_s}[f(x_i,y_j)-\bar{f}]^2}\sqrt{\Sigma_{i=1}^{m_s}\Sigma_{j=1}^{m_s}[g(x_i^*,y_j^*)-\bar{g}]^2}} \quad (1)$$

Here, $f(x,y)$ is the gray level value at coordinates (x,y) for the original image, $g(x^*, y^*)$ is the gray level value at coordinates (x^*, y^*) for the target image, C is the maximum correlation factor, $\bar{f}$ and $\bar{g}$ are the average gray values of the image $f(x,y)$ and $g(x^*, y^*)$, respectively. The correlations between the coordinates (x, y) and (x^*, y^*) are established by the deformation which occurred between two images. If the motion of the object relative to the camera is parallel to the image plane, the relationship between the coordinates (x, y) and (x^*, y^*) can be expressed as:

$$\begin{cases} x^* = x + u + \Delta x\frac{\partial u}{\partial x} + \Delta y\frac{\partial u}{\partial y}, \\ y^* = y + v + \Delta x\frac{\partial v}{\partial x} + \Delta y\frac{\partial v}{\partial y}. \end{cases} \quad (2)$$

where u and v are the displacement component for the subset centers in the x and y directions, respectively. The term Δx and Δy are the distances from the subset center to the point (x, y). Digital image correlation technology is used to obtain six deformation parameters for u, v, $\partial u/\partial x$,$\partial v/\partial y$,$\partial u/\partial y$, and $\partial v/\partial x$. The displacement and strain with the maximum C are considered the true displacement and strain. In this method, the measurement precision will reach 0.05 pixels.

In using DSCM, the specimen surface is usually sprayed with black and white paint to form a random pattern. This pattern was applied by first coating the surface with white paint and then allowing the overspray from a can of black paint to speckle the white surface. It is easy to find the image pairs of this kind of black and white pattern using digital image correlation method.

APPLICATION OF DSCM IN FGM FRACTURE MECHANICS

Preparation and characterization of FGM

In this study, photodegradable method was used to fabricate the functionally graded polymethyl methacrylate (PMMA) material. The specific method and principle of UV irradiation are described in detail.[22] In order to make graded variations of the mechanical properties along the width of the specimen, a special experimental electronic apparatus was designed including a precise motor, a plane table, and a computer with control software. It could be automatically moved at a uniform speed. The electronic control system was used to perform a slow rotation. The strips with nominally 100 mm length, 40 mm width, and 1 mm thickness were placed on the experimental table, moved along the width direction of the specimen at a very slow speed of 0.01 m/h. Under the irradiation of UV light, the motion of the specimen resulted in different irradiation times. Finally, the gradient variation of elastic modulus along the width direction of the specimen can be achieved according to the design requirement. The final FGM specimen is shown in Figure 2. In this study, the elastic modulus of the material is regarded as linear variation.

Two kinds of gradient materials and one homogeneous material are prepared as shown in Figure 3.

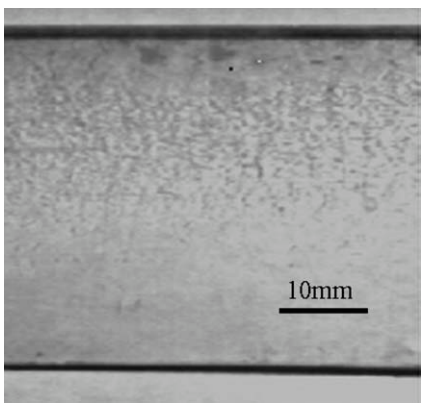

Figure 2 Gradient PMMA using UV irradiation.

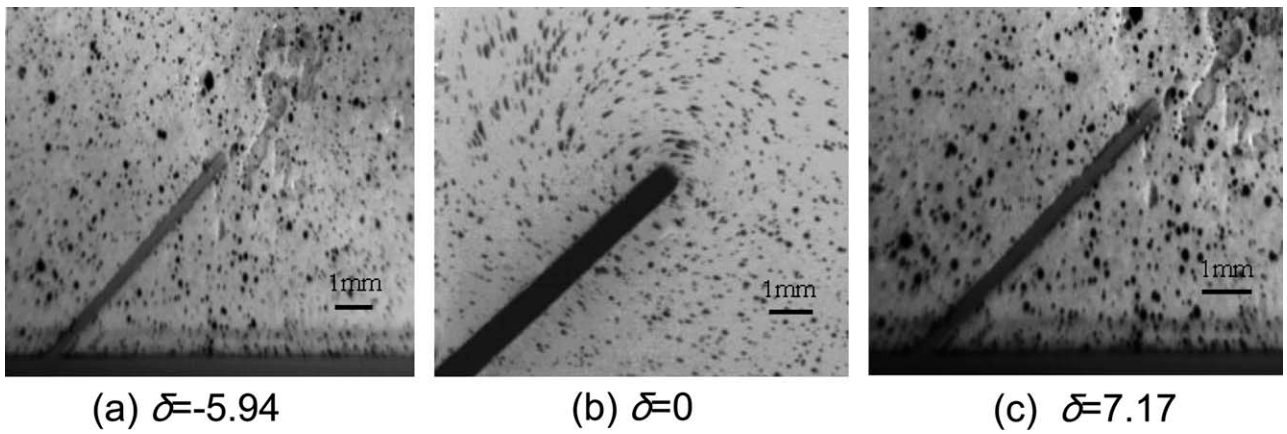

Figure 3 Speckle pattern of specimens with different gradient coefficients.

The elastic modules of three different materials can be expressed as:

$$\begin{aligned} E &= 3.04(1 - 5.94x_1)\ \textbf{GPa} \qquad \delta < 0, \\ E &= 2.42(1 + 0.00x_1)\ \textbf{GPa} \qquad \delta = 0, \\ E &= 2.51(1 + 7.17x_1)\ \textbf{GPa} \qquad \delta > 0. \end{aligned} \tag{3}$$

Here x_1 is the coordinate value on the width direction of the sample. An initial 45° edge crack (crack-tip radius 0.15 mm) with 0.3 mm width and 7 mm length is cut in the middle position of bottom side in each specimen using a high-speed diamond impregnated circular saw. In FGM, δ is the gradient parameter, the gradient direction is parallel to the width direction of the specimen.

Both the crack-tip coordinates and the gradient variation can be seen in Figure 4. E_0 is the elastic modulus at the crack tip, E_1 and E_2 are the elastic modulus at both sides of the specimen, respectively. The first specimen is the crack on the stiff side of the material while being loaded on the compliant side ($E_2/E_1 < 1$, $\delta = -5.94$). The second specimen is a homogenous material with the same elastic modulus ($E_2/E_1 = 1$, $\delta = 0$). The third specimen is about the crack on the compliant side and being loaded on the stiff side ($E_2/E_1 > 1$, $\delta = 7.17$). Both the coordinate (x, y) and (x_1, y_1) are Cartesian coordinates at the crack tip, and (r,θ) is a polar coordinate. In coordinate system (x_1, y_1), x-axis and y-axis are parallel to the vertical and horizontal sides of the specimen, respectively. The material gradient direction is along the x_1-axis. The angle between the gradient direction and the crack is φ which is assumed to be $-\pi/2 < \varphi < \pi/2$. On the other hand, artificial speckle can be made through spraying black/white paint on the surface of the specimens. In this experiment, speckle fields of three kinds of specimens are shown in Figure 3.

Considering the difficulty of the specimen preparation, the cracked specimen with $\varphi = 45^\circ$ is chosen. The specimen was loaded using the tensile machine. The applied load is measured using the force sensor. During the whole experimental process, speckle photos under different loads are taken accordingly. Displacement fields (u_1, v_1) in the global coordinates (x_1, y_1) can be obtained, and the contours of the displacement fields are in comparison with finite elements results.

Fracture mechanics of FGM

According to the relationship of the coordinates in Figure 4, the displacement fields in the crack-tip coordinates can be expressed as:

$$\begin{aligned} u &= (u_1 - u_{10})\cos\varphi - (v_1 - v_{10})\sin\varphi, \\ v &= (v_1 - v_{10})\cos\varphi + (u_1 - u_{10})\sin\varphi. \end{aligned} \tag{4}$$

Here, (u_{10}, v_{10}) are the displacements at the crack tip in the global coordinates, φ is the angle between the local coordinates (x, y) and the global coordinates (x_1, y_1).

According to Erdogan's suggestion,[23] only the elastic constants near the crack-tip are considered, thus:

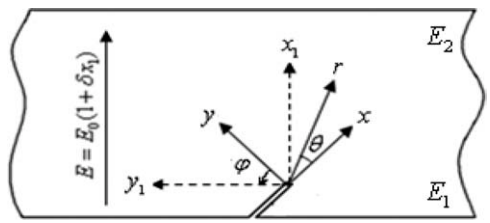

Figure 4 Tip coordinates of mixed-mode crack.

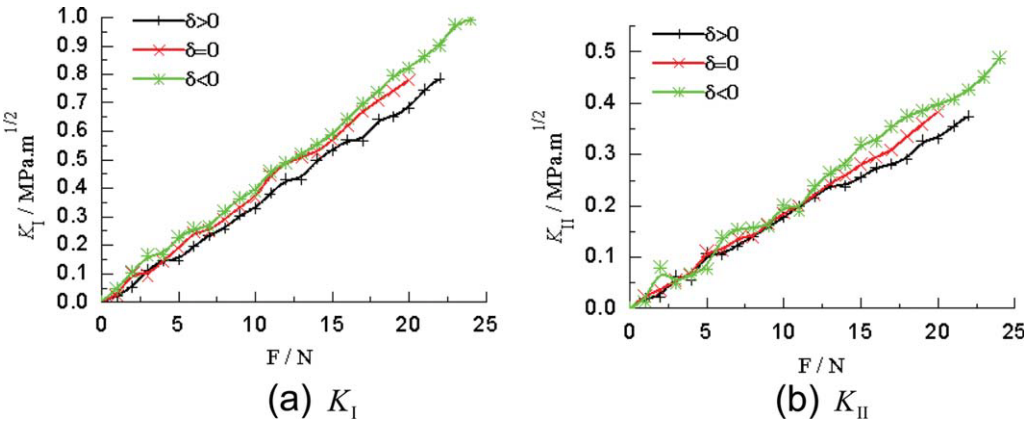

Figure 5 Stress intensity factors of graded materials with different gradient coefficients. [Color figure can be viewed in the online issue, which is available at wileyonlinelibrary.com.]

$$u = \frac{K_I}{4G_0}\sqrt{\frac{r}{2\pi}}\left[(2k-1)\cos\frac{\theta}{2} - \cos\frac{3\theta}{2}\right] + \frac{K_{II}}{4G_0}\sqrt{\frac{r}{2\pi}}\left[(2k+3)\sin\frac{\theta}{2} + \sin\frac{3\theta}{2}\right],$$
$$v = \frac{K_I}{4G_0}\sqrt{\frac{r}{2\pi}}\left[(2k+1)\sin\frac{\theta}{2} - \sin\frac{3\theta}{2}\right] - \frac{K_{II}}{4G_0}\sqrt{\frac{r}{2\pi}}\left[(2k-3)\cos\frac{\theta}{2} + \cos\frac{3\theta}{2}\right]. \quad (5)$$

Here, K_I and K_{II} are the mode I and mode II stress intensity factors near the crack-tip, respectively; G_0 is the shear module at the crack tip; k is the elastic constant, for plane stress conditions, $k = (3 - \nu)/(1 + \nu)$, and for plane strain conditions, $k = 3 - 4\nu$. ν is the Poisson's ratio of the material. In this study, the plane stress condition is selected.

For the problem of mixed-mode cracks, two stress intensity factors K_I and K_{II} can be obtained from the displacement fields in eq. (5). Since large errors may be found in calculating K_I and K_{II} due to the sharp variation of the displacements near the crack-tip, some changes must be made in eq.(5). Considering the symmetry of trigonometric function, eq. (5) becomes:

$$K_I = \frac{2G_0(v(r,\theta) - v(r,-\theta))}{(2k+1)\sin\frac{\theta}{2} - \sin\frac{3\theta}{2}}\sqrt{\frac{2\pi}{r}},$$
$$K_{II} = \frac{2G_0(u(r,\theta) - u(r,-\theta))}{(2k+3)\sin\frac{\theta}{2} + \sin\frac{3\theta}{2}}\sqrt{\frac{2\pi}{r}}. \quad (6)$$

RESULTS AND DISCUSSIONS

Influence of gradient coefficient on stress intensity factors

Several pairs of points (r_i, θ_i),$(r_i, -\theta_i)$ ($\theta_i > 0$, $i = 1,2,\ldots,n$) are selected in the K-dominant stress fields, and the in-plane displacements $(u_{1i}(r, \theta), v_{1i}(r, \theta))$ and $(u_{1i}(r, -\theta), v_{1i}(r, -\theta))$ at $2k$ positions in the global

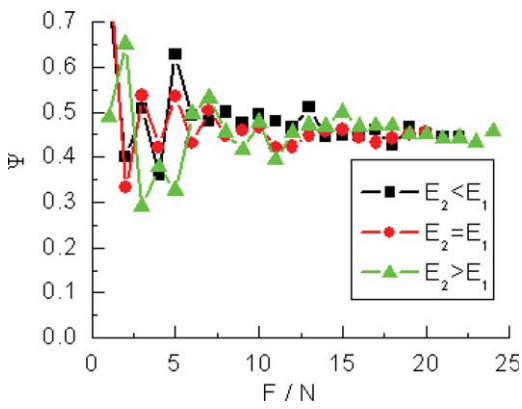

Figure 6 Curves of relationship between Ψ and F. [Color figure can be viewed in the online issue, which is available at wileyonlinelibrary.com.]

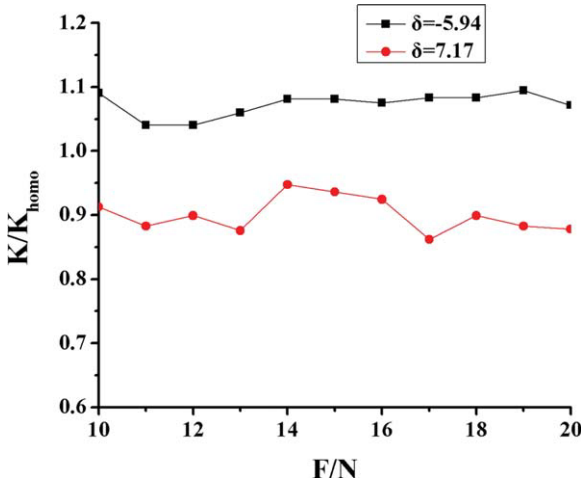

Figure 7 K/K_{homo} for materials with different gradient coefficients. [Color figure can be viewed in the online issue, which is available at wileyonlinelibrary.com.]

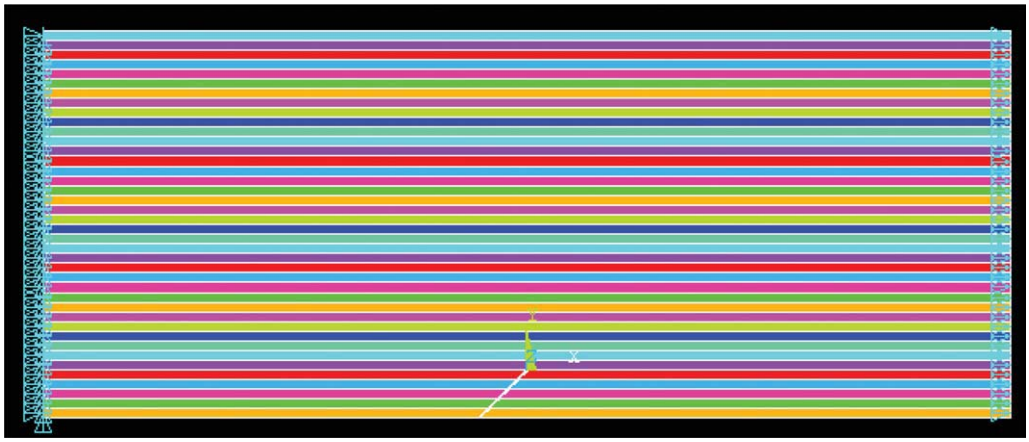

Figure 8 Finite element model of mixed-mode crack under constant displacement tension. [Color figure can be viewed in the online issue, which is available at wileyonlinelibrary.com.]

coordinates are obtained, so the displacements ($u_i(r, \theta)$, $v_i(r, \theta)$)and ($u_i(r, -\theta)$, $v_i(r, -\theta)$) in the crack-tip coordinates can be deduced. The stress intensity factors corresponding to each pair of points can be calculated out using eq. (6), and the nearest value to the real stress intensity factors can be obtained using the least square method.

According to eqs. (3)–(6), the relationships between the stress intensity factors K_I, K_{II} and the applied load for three different specimens are plotted in Figure 5, respectively. The nearly linear relationships between the stress intensity factors and the loads are found before three kinds of samples were ruptured, which indicated that the materials are almost linear elastic until fractured. Plastic influences can be ignored and it is reasonable to treat this as linear elastic fracture problems.

According to Figure 5, as $\delta < 0$, the stress intensity factors K_I, K_{II} are the largest, and as $\delta > 0$, the stress intensity factors K_I, K_{II} are the smallest. With increasing gradient parameter, the stress intensity factors decrease. Under the premise of K-dominance, the specimen with a crack on the stiff side ($E_2/E_1 < 1$, $\delta < 0$) experienced lower value of K_I and K_{II} when compared with that of the homogenous specimen ($\delta = 0$) subjected to the identical far-field loading. On

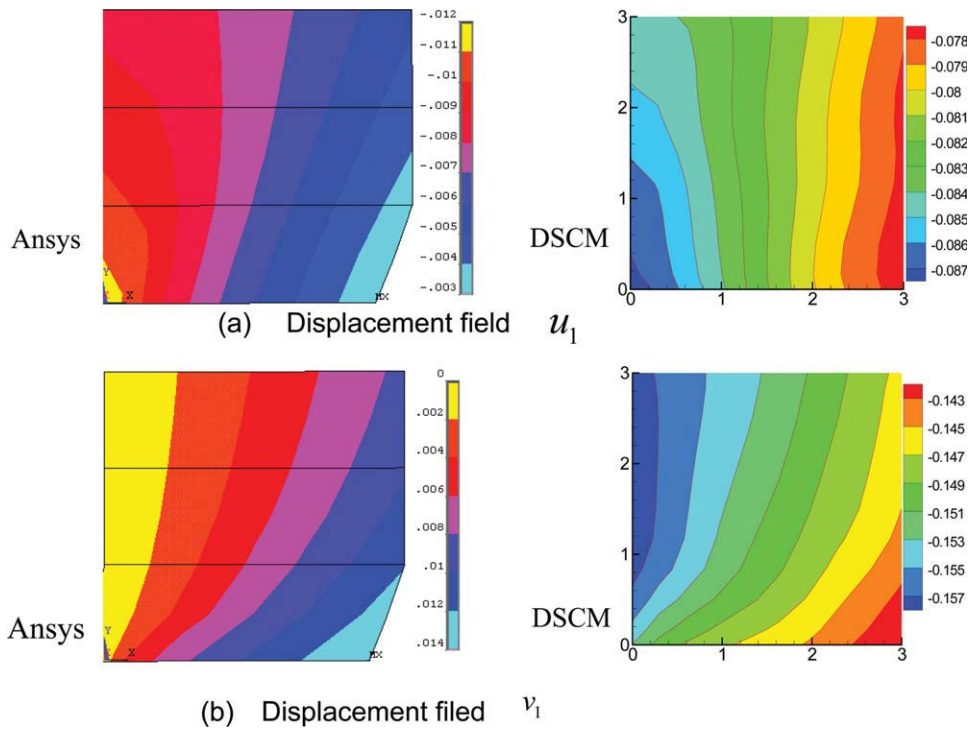

Figure 9 Crack tip displacement fields as $\delta = -5.94$. [Color figure can be viewed in the online issue, which is available at wileyonlinelibrary.com.]

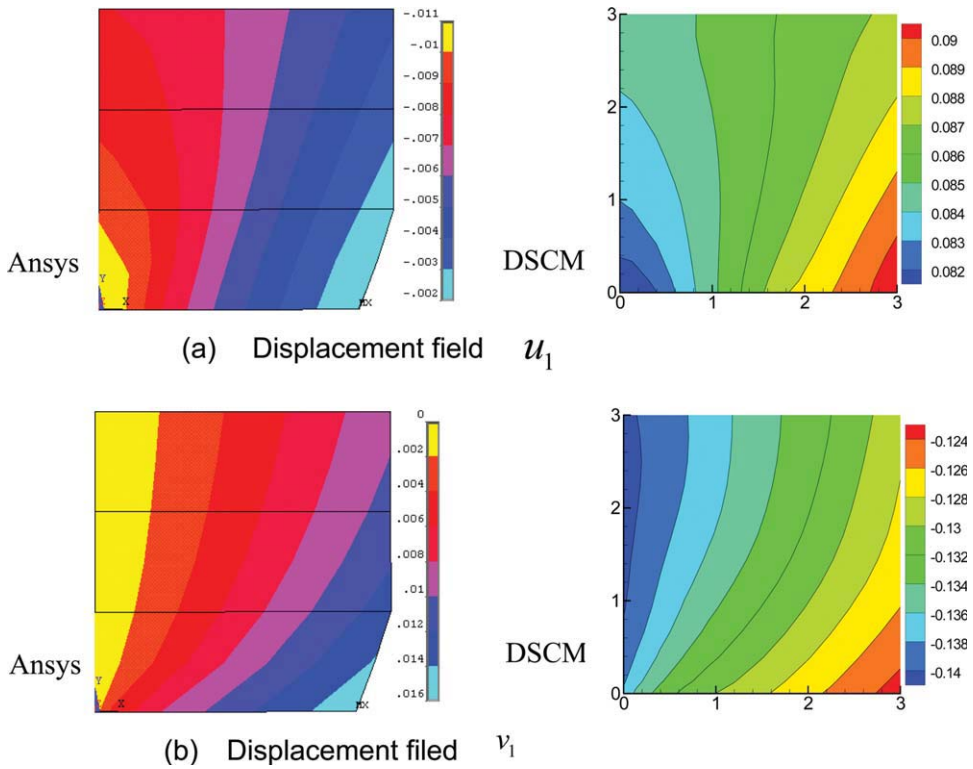

Figure 10 Crack tip displacement fields as $\delta = 0$. [Color figure can be viewed in the online issue, which is available at wileyonlinelibrary.com.]

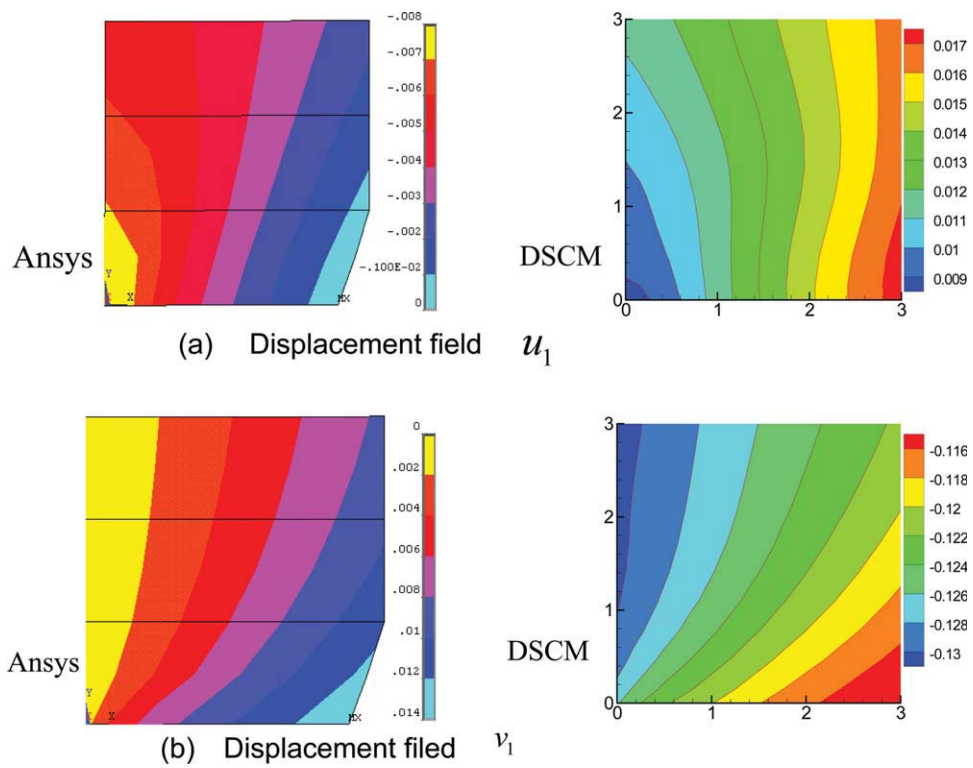

Figure 11 Crack tip displacement fields as $\delta = 7.17$. [Color figure can be viewed in the online issue, which is available at wileyonlinelibrary.com.]

TABLE I
Both the Crack Tip Displacement and Far Field Displacement

	FEM			DSCM		
	Crack tip displacement	Far field displacement	Relative displacement	Crack tip displacement	Far field displacement	Relative displacement
$\delta = -5.94$						
u	−0.012	−0.003	−0.009	−0.087	−0.078	−0.009
v	0	0.014	−0.014	−0.155	−0.143	−0.012
$\delta = 0$						
u	−0.011	−0.002	−0.009	0.082	0.09	−0.008
v	0	0.016	−0.016	−0.14	−0.124	−0.016
$\delta = 7.17$						
u	−0.008	0	−0.008	0.009	0.017	−0.008
v	0	0.014	−0.014	−0.128	−0.116	−0.012

the contrary, the specimen with a crack on the compliant side ($E_2/E_1 > 1$, $\delta > 0$) has higher value of K_I and K_{II} than that of the homogenous specimen ($\delta = 0$). This suggests that elastic gradients shield a crack on the stiff side under loading condition.

Influence of gradient coefficient on fracture mode

In order to discuss the fracture properties of graded materials conveniently, the stress intensity factor is expressed in complex formulation $\bar{K} = K(\cos\Psi + i\sin\Psi)$, here $K = \sqrt{K_I^2 + K_{II}^2}$, $\Psi = \arctan(K_{II}/K_I)$, and the influence of φ and δ on K and Ψ will be investigated. The K indicates the material fracture capability, and the Ψ indicates the crack mode.

As $\varphi = \pi/4$, the variations of Ψ depending on the load are shown in Figure 6 for three specimens with different gradient coefficients. As the load is small, due to the error resulting from DSCM itself, the variations of Ψ is not in order. As the load increases to 10 N, the variations of Ψ become steady. As the load becomes large than 15 N, the Ψ almost reach to a constant 0.45. It can be deduced that the crack mode is not dependent on the gradient coefficient δ.

In this article, elastic module of the crack tip are different for the specimen with the gradient coefficients −5.94 and 7.17, respectively. The material fracture capability cannot be evaluated by comparing the stress intensity factors (SIF) directly. It is necessary to examine the SIF in graded materials in comparison with the SIF of corresponding homogeneous materials. Figure 7 shows that, there are $K/K_{homo} > 1$ as $\delta = -5.94$, and $K/K_{homo} < 1$ as $\delta = 7.17$, here K_{homo} is the stress intensity of the corresponding homogeneous material. It indicates that the material facture capability will depend on the gradient coefficient, and the positive graded coefficient is more favorable.

Comparison of fracture behaviors between FEM simulation and DSCM experiment

FEM software (Ansys) is used to simulate the fracture characterizations of the FGMs. The finite elements model of the mixed-mode crack is shown in Figure 8. The specimen is divided into 40 layers along the width. The variation of the elastic module is denoted by different colors in Figure 8. One end of the specimen is fixed, and the displacement of the other end is u. Solid 95 unit is adopted, and there are totally 32,060 units and 178,655 nodes.

The crack opening displacements are used to obtain the stress intensity factors. As $\theta = \pi$ in eq. (6), it has

$$K_I = \frac{G_0(v(r,\pi) - v(r,-\pi))}{1+k}\sqrt{\frac{2\pi}{r}},$$
$$K_{II} = \frac{G_0(u(r,\pi) - u(r,-\pi))}{1+k}\sqrt{\frac{2\pi}{r}}. \quad (7)$$

As r is small enough, K_I and K_{II} in eq. (7) will approximate to be two constants, which are considered to be the real stress intensity factors at the crack-tip.

As an example, the displacement fields (u_1, v_1) in the whole coordinates (x_1, y_1) are figured out using digital correlation speckle method and finite elements modeling as shown in Figures 9–11. Both the crack tip displacement and far field displacement are summarized as shown in Table I. In view of rigid motion of DSCM experiment, the relative displacements are also shown in Table I.

It is obvious that the trends of displacement fields in homogeneous materials obtained from the digital speckle experiment coincide with finite elements simulation results in Figures 9–11. For graded materials, the trends of v_1 obtained from experiment results and finite elements results are almost the same, and the trends of u_1 are slightly different, but the whole trends are the same. The displacements of homogeneous materials are slightly larger than those

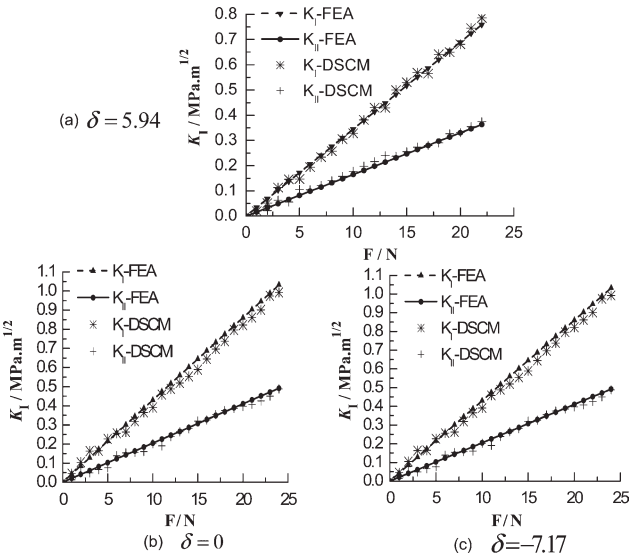

Figure 12 Comparison between FEM and DSCM results.

of two graded materials due to the elastic modulus increasing after being irradiated. The comparison between finite elements simulation results and digital speckle results are shown in Figure 12. A good coincidence of crack tip stress intensity factors can be found and the errors are within 10%. The results from finite elements simulation in Table II show the influences of the angle φ between the gradient direction and the crack and gradient coefficients δ on the crack tip stress intensity factors K and crack modes Ψ. For all crack modes, the stress intensity factor K decreases with the increasing of gradient coefficient δ. The positive gradient coefficients δ result in less stress intensity factors. The crack mode Ψ is almost not changed, which indicates that the influence of the gradient coefficient on the crack mode is negligible. All of the above FEM results coincide with the experimental results.

TABLE II
Comparison of FEM Results Between Mode I (φ = 0) Crack and Mixed Mode Crack (φ = 0)

φ	δ	K (MPam$^{1/2}$)	Ψ	K/K_{homo}
0	−24	1.532	0	1.692818
	−12	1.144	0	1.264088
	−6	1.012	0	1.118232
	0	0.905	0	1
	6	0.817	0	0.902762
	12	0.743	0	0.820994
	24	0.625	0	0.690608
π/6	−24	1.460	0.348	1.693735
	−12	1.090	0.348	1.264501
	−6	0.964	0.347	1.118329
	0	0.862	0.347	1
	6	0.777	0.346	0.901392
	12	0.707	0.346	0.820186
	24	0.594	0.345	0.689095
π/4	−24	1.358	0.501	1.693267
	−12	1.015	0.500	1.265586
	−6	0.897	0.499	1.118454
	0	0.802	0.498	1
	6	0.723	0.497	0.901496
	12	0.657	0.497	0.819202
	24	0.553	0.495	0.689526
π/3	−24	1.169	0.629	1.691751
	−12	0.873	0.628	1.263386
	−6	0.772	0.627	1.117221
	0	0.691	0.626	1
	6	0.623	0.625	0.901592
	12	0.567	0.624	0.82055
	24	0.477	0.622	0.690304

CONCLUSIONS

In combination with finite elements method, the digital speckle experimental methods are used to investigate the influence of gradient coefficients on the fracture behavior of graded materials. The following conclusions are obtained:

1. Under the premise of K-dominance, the specimen with a crack on the stiff side ($E_2/E_1 < 1$, $\delta < 0$) experienced lower value of K_I and K_{II} when compared with that of the homogenous specimen ($\delta = 0$) subjected to the identical far-field loading. On the contrary, the specimen with a crack on the compliant side ($E_2/E_1 > 1$, $\delta > 0$) has higher value of K_I and K_{II} than that of the homogenous specimen ($\delta = 0$). This suggests that elastic gradients shield a crack on the stiff side under loading condition.
2. The displacement fields (u_1, v_1) in the whole coordinates (x_1, y_1) for different FGMs are compared using digital correlation speckle method and finite elements modeling. The corresponding stress intensity factors at crack tip are extracted. The results reveal that the fracture capabilities of the crack in graded materials are influenced by the gradient coefficients.
3. The influences of gradient coefficients on fracture modes are not noticeable. For any gradient coefficient, the phase angle Ψ of the mixed-mode stress intensity factors becomes a constant gradually with the increasing of the applied load.

References

1. Suresh, S. Science 2001, 292, 2447.
2. Yao, X. F.; Xu, W.; Bai, S. L.; Yeh, H. Y. Compos Sci Technol 2008, 68, 953.
3. Xu, H. M.; Yao, X. F.; Feng, X. Q.; Yeh, H. Y. Compos Sci Technol 2008, 68, 27.
4. Xu, H. M.; Yao, X. F.; Feng, X. Q.; Hisen, Y. Y. Mech Mater 2008, 40, 37.
5. Yao, X. F.; Yeh, H. Y.; Chen, X. B. Model Simul Mater Sci 2005, 13, 621.

6. Butcher, R. J.; Rousseau, C. E.; Tippur, H. V. Acta Mater 1998, 47, 259.
7. Rousseau, C. E.; Tippur, H. V. Acta Mater 2000, 48, 4021.
8. Gu, P.; Dao, M.; Asaro, R. J. J Appl Mech-T ASME 1999, 66, 101.
9. Anlas, G.; Santare, M. H.; Lambros, J. Int J Fract 2000, 104, 131.
10. Ma, Y. J.; Yao, X. F.; Zheng, Q. S.; Yin, Y. J.; Jiang, D. J.; Xu, G. H.; Wei, F.; Zhang, Q. A. Appl Phys Lett 2010, 97, 061909.
11. Yao, X. F.; Zhou, D.; Yeh, H. Y. Aerosp Sci Technol 2008, 12, 223.
12. Yamaguchi, I. J Phys E Sci Instrum 1981, 14, 1270.
13. Peters, W. H.; Ranson, W. F. Opt Eng 1982, 21, 427.
14. Chu, T. C.; Ranson, W. F.; Sutton, M. A.; Peters, W. H. Exp Mech 1985, 25, 232.
15. Bruck, H. A.; McNeill, S. R.; Sutton, M. A.; Peters, W. H. Exp Mech 1989, 29, 261.
16. Jin, G. C.; Wu, Z.; Bao, N. K.; Yao, X. F. Opt Laser Eng 2003, 39, 457.
17. Meng, L. B.; Jin, G. C.; Yao, X. F. Opt Laser Eng 2007, 45, 57.
18. Meng, L. B.; Jin, G. C.; Yao, X. F.; Yeh, H. Y. Polym Test 2006, 25, 42.
19. Yao, X. F.; Meng, L. B.; Jin, J. C.; Yeh, H. Y. Polym Test 2005, 24, 245.
20. Sutton, M. A.; Turner, J. L.; Bruck, H. A.; Chae, T. A. Exp Mech 1991, 31, 168.
21. Jin, X.; Wu, L. Z.; Guo, L. C.; Yu, H. J.; Sun, Y. G. Eng Fract Mech 2009, 76, 1800.
22. Yao, X. F.; Liu, D. L.; Yeh, H. Y. J Appl Polym Sci 2007, 106, 3253.
23. Erdogan, F. Compos Eng 1995, 5, 753.